ECLÉTICA Química

Volume 28 (2003) número 2

Editora UNESP

www.scielo.br/eq

Electrochemical and physical characterization of Ni-Cu-Fe alloy for chlor-alkali hydrogen cathodes

*M. J. Giz[1] *, M. C. Marengo[1], E. A. Ticianelli[1], E. R. Gonzalez[1]*

[1]Instituto de Química de São Carlos – USP – CEP 13560-970 - São Carlos-SP-Brasil

Abstract: This work describes the development of an alternative acetate bath for the electrochemical codeposition of Ni-Cu-Fe electrodes at low pH that is stable for several weeks and produces electrodes with good performance for chlor-alkali electrolysis. Physical characterization of the electrode surface was made using X ray absorption spectroscopy (XAS), scanning electron microscopy (SEM) and energy dispersive analysis (EDX). The evaluation of the material as electrocatalyst for the hydrogen evolution reaction (*her*) was carried out in brine solution (160 g L^{-1} NaCl + 150 g L^{-1} NaOH) at different temperatures through steady-state polarization curves. The Ni-Cu-Fe electrodes obtained with this bath have shown low overpotentials for the *her*, around 0.150 V at 353 K, and good stability under continuous long-term operation for 260 hours. One positive aspect of this cathode is that the polarization behavior of the material shows only one Tafel slope over the temperature range of 298 – 353 K.

Keywords: hydrogen production; cathodes; electrolysis; chlor-alkali.

Introduction

Hydrogen is one of the most promising energy carriers that can be an alternative to fossil fuels. In industrial electrolytic cells, the formation of H_2 can arise either as the desired product in the case of water electrolysis or as a by product, e.g. as in the chlor-alkali process or in chlorate production. The cost of this hydrogen is still too high compared to that of the hydrogen obtained by reforming from hydrocarbon sources. There is no doubt that the electricity cost is the largest factor contributing to the cost of the electrolytic production of hydrogen, and it varies with the cell voltage. Adequate electrolyser hardware design and operation allow a reduction of the cell voltage and thereby the production costs.

In order to improve the electrolytic hydrogen production process, many attempts have been made to develop efficient and durable electrode materials for the hydrogen evolution reaction (*her*) in alkaline solutions[1]. Nickel based electrodes are amongst the more active electrode materials for the *her* in alkaline solutions[1-7]. A combination of a large surface area with an enhanced catalytic activity, enables codeposits of Ni with other metals such as Co, Zn or Fe, to operate at overpotentials for the *her* close to 100 mV, well below the value of ~ 400 mV typically observed under industrial conditions[5-7].

It is known that the electrocatalytic activity for the *her* on metal and alloy electrodes is closely related to their surface and/or electronic properties[8]. In fact, several attempts have been made to relate the electrocatalytic activity of metals and alloys to their electronic structures[9]. Among several other methods, X-ray absorption spectroscopy (XAS) is a suitable tool to access important aspects of the electronic, geometric, and surface properties of pure metals and metal alloys. Studies of X-ray absorption have been carried out on platinum and platinum based alloys directed to the electrocatalysis of the oxygen reduction and

* E-mail address: mjgiz@iqsc.sc.usp.br

hydrogen oxidation reactions in acid media, which are important processes for several fuel cell technologies [10-11]. Strong effects on the electronic charges in the Pt-Pt bond introduced by Ru, Sn, Cr, V, Co, etc., were observed in these studies. Metal hydride electrodes of the type AB_5 for nickel-metal hydride batteries have also been studied [12-14]. It has been found that a larger Ni *d* band vacancy is beneficial to increase the amount of hydrogen stored in metal hydride alloys [12-14]. For the nickel electrode, very important information regarding the structure and electronic distribution on several kinds of nickel hydrous oxides has been reported [15-16]. These studies showed that XAS is a very suitable technique for the study of catalysts, particularly to understand the role of the electronic structure, the environment surrounding minor constituents, and corrosion processes of the individual components.

Previous works conducted in this laboratory [3,4] have shown that Ni-Fe codeposits, after activation by partial oxidation in acid medium, present an enhanced activity for the *her* in strongly alkaline solutions. In those works, Ni-Fe codeposits were electroplated on mild steel using different electrodeposition baths and evaluated for the *her* in both water and chlor-alkali electrolysers. The Ni-Fe codeposits were found to have a good performance for the *her* for long-term operation, but the stability of the plating bath was very poor particularly, due to a predominant precipitation of $Fe(OH)_2$. This causes a rapid loss of bath activity resulting in higher costs for industrial application. In this work, a modified and optimized bath that is stable for several weeks without loss of the electrocataytic properties was developed for the preparation of Ni-Cu-Fe electrodeposits. Electrochemical studies were carried out by steady-state polarization measurements. X-ray absorption spectroscopy studies of the electrochemical codeposits were done to characterize the electronic (from x-ray near edge structure, XANES) and structural (from extended x-ray absorption fine structure, EXAFS) parameters of the metal codeposits with element specificity.

Experimental

The electrodepositions of Ni-Cu-Fe were carried out on mild steel substrates having an exposed area of 0.5 cm^2. The composition of the steel (apart from Fe) was: C= 0.102%, Si=0.05%, Mn=0.62%, P=0.09%, S=0.019% and Mg=0.016%. Before each electrodeposition, the surface of the substrate was polished with emery paper, treated in 10% HCl solution, and cleaned in pure water. Ni, Cu and Fe were codeposited from an acetate bath containing 130 g L^{-1} of $Ni(CH_3COO)_2$; 10 g L^{-1} of $FeSO_4$; 0.22 g L^{-1} of $Cu(OOCCH_3)_2$; 25 g L^{-1} of H_3BO_3 and 0.75 mL L^{-1} of $HCONH_2$, under the following conditions: current density = 25 mA cm^{-2}, temperature = 318 K, deposition time = 60 min, pH 3.2, counter electrode = nickel foil, with continuous stirring. After the depositions, the electrodes were partially activated in a 10% HCl v/v solution, by applying an anodic current density of 12 mA cm^{-2} for 15 seconds.

For the XAS experiments, the Ni-Cu-Fe alloy samples were prepared using the same conditions for the codeposition of the metals, but on thin porous carbon paper substrates. Also an eletroctroplated Ni obtained from a Watts bath (300 g/L of $NiSO_4.6H_2O$, 45 g/L $NiCl_2.6H_2O$ and 30 g/L of H_3BO_3) was prepared for comparison. The load of Ni metals in the carbon paper was of the order of 5 mg cm^{-2}.

The electrochemical measurements were carried out in a three-compartment cell under galvanostatic steady state conditions. A platinum foil was used as auxiliary electrode and an Hg/HgO/OH^- system was used as reference electrode linked to the working compartment via a Luggin capillary. A Potentiostat/Galvanostat PAR model 273A with iR compensation was used to record the polarization curves. The electrolyte solution was a mixture of 150 g dm^{-3} of NaOH + 157 g dm^{-3} of NaCl, called here "brine solution". The working solutions were prepared with p.a. reagents and water purified in a Milli-Q (Milli Pore) system.

The surface morphology of the Ni-Cu-Fe electrodes was analyzed by Scanning Electron Microscopy (SEM) using a ZEISS DSM 960 equipment. The Ni and Fe contents were determined by Energy Dispersive X-ray (EDX) analyses with a LIMK QX 2000.

The X-ray absorption data were collected in the transmission (Ni and Fe metals in the reference foils and Ni in the samples) and fluorescence (Fe in the Ni-Cu-Fe samples) modes in the K edge of Ni and Fe. Measurements were conducted at the XAS

beam line of the LNLS - National Synchrotron Light Source, Brazil. The data acquisition system for XAS comprised three ionization detectors (incidence I_o, transmitted I_t, and reference I_r) and a fluorescence detector. The reference channel was employed primarily for internal calibration of the edge positions by using pure foils of the elements. Air was used in the I_o, I_t, and I_r chambers. Owing to the low critical energy of the LNLS storage ring (2.08 keV), third order harmonic contamination of the Si(111) monochromatic beam is expected to be negligible above 5 keV [17].

The computer program used for the analysis of the X-ray absorption data was the WinXAS package [18]. The data analysis was done according to procedures described in detail in the literature [12,19]. Briefly, the XANES spectra were first corrected for background absorption by fitting the pre-edge data (from -60 to -20 eV below the edge) to a linear formula, followed by extrapolation and subtraction from the data over the energy range of interest. Next, the spectra were calibrated for the edge position using the second derivative of the inflection point at the edge jump of the data from the reference channel. Finally, the spectra were normalized, taking as reference one of the inflection points of the EXAFS oscillations. The EXAFS oscillations were removed from the measured absorption coefficient by using a cubic spline background subtraction. Next, the EXAFS were normalized, that is, converted to signal per absorbing atom dividing by the height of the absorbing edge given by the fitted spline function. Fourier transforms of the EXAFS oscillations were obtained employing the Hanning window, k^2 weight, and the Dk values were specified in the corresponding Figures.

Results and discussion

In order to improve the stability of the plating bath, Ni-Cu-Fe electrodeposits were prepared using plating solutions with different pHs, 1.2, 2.2, 3.2 and 5.2 while all other conditions were maintained the same as reported previously [4]. In all cases, except for pH 5.2, no evidence of precipitated iron hydroxide just after the electrodepositions were detected from visual analysis of the baths. In fact, a pH of 5.2 represents the unstable bath condition reported previously [4] for the preparation of Ni-Fe electrodeposits. Electrochemical tests have shown that the best electrocatalytic activity for the HER was obtained for the material prepared with the bath at pH 3.2. The comparison of the electrochemical behavior of the electrode materials obtained with the baths at pH 3.2 and 5.2 showed that the overpotential at a current density of 210 mA cm^{-2} for the first electrode was ~ 40 mV above the value obtained for the second one. As the properties of the electrodeposited material are very dependent on the electrodeposition parameters, these were also optimized to lower the overpotential for the *her* on the produced material. Thus, for a bath with pH 3.2, the best conditions found were a current density of 20 mA cm^{-2} and 60 minutes of electrodeposition time.

Physical Characterization

The chemical composition of the electrodeposits prepared with a bath with pH 3.2, under optimized conditions, was determined by EDX analysis and it was found that the Ni-Cu-Fe surface composition is Ni = 49, Cu = 43 and Fe = 8 atoms %. This result is very surprising and intriguing because of the high content of copper that appears homogenously distributed in the electrodeposit in spite of the very low concentration of the precursor in the electrodeposition bath. It is highly probable that the deposition of copper could be inhibiting the deposition of iron and resulting in the low content of this element (8 atom %). Because of this result the codeposition of Ni, Cu and Fe in the given bath can be classified as anomalous.

Figure 1 presents a scanning electron micrograph with a magnitude of 10000x for the Ni-Cu-Fe surface just after the electrodeposition. It is observed a very rough surface with a cauliflower structure indicating that the electrodeposit has a larger area when compared with just the Ni-Fe material obtained by Carvalho et al.[4]

XANES spectra contain information on the local atom symmetry and density of states of metals and alloys. Figures 2 and 3 show XANES spectra obtained at the Ni and Fe K edges, respectively, for the electroplated Ni and Ni-Cu-Fe electrodeposits and in Figure 4 the

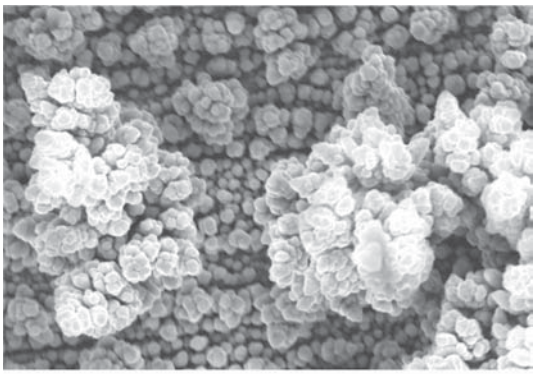

Figure 1. Scanning electron micrograph of the Ni-Cu-Fe electrodeposit. 10000x.

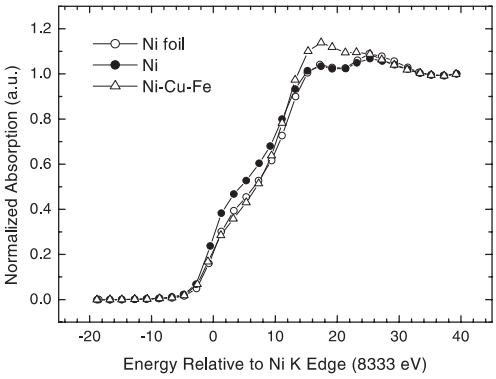

Figure 3. XANES spectra at the Fe K edges: Fe foil, FeOOH, and Ni-Cu-Fe alloy.

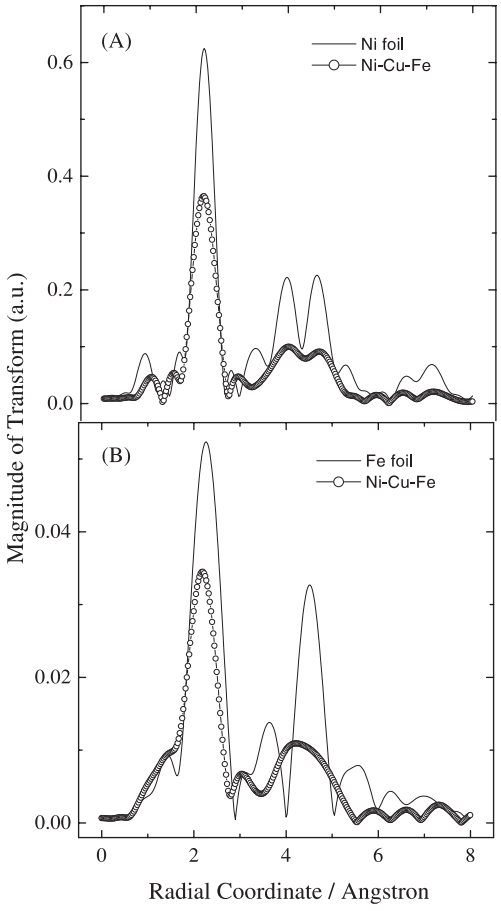

Figure 2. XANES spectra at the Ni K edges: Ni foil; electroplated Ni and Ni-Cu-Fe alloy.

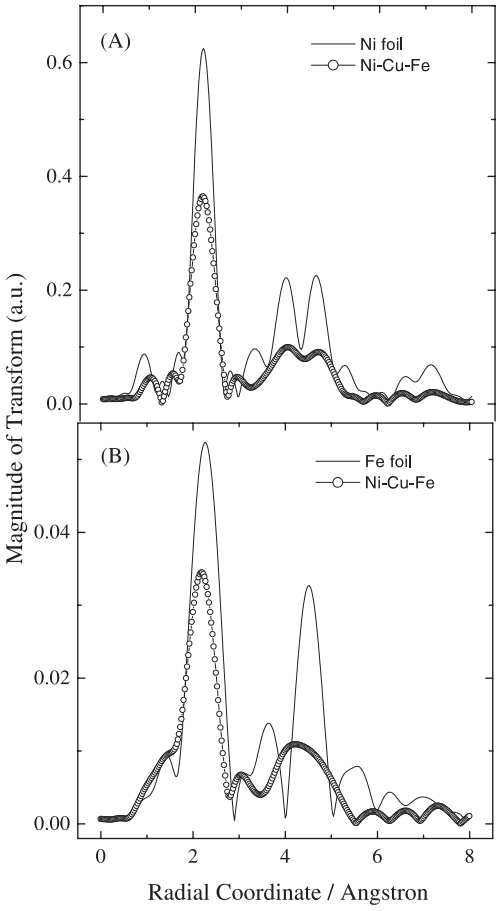

Figure 4. EXAFS signal at Ni (A) and Fe (B) K edges: Ni (Dk = 3.99 - 12.51) and Fe (Dk = 4.18 - 11.12); Ni-Cu-Fe (A: Dk =3.97 - 12.13; B: Dk = 3.98 - 11.12).

corresponding results of the Fourier transform of the EXAFS signals are shown. Results for Ni and Fe foil are included for comparison.

It is seen that at both Ni and Fe K edges the XANES spectra present an absorption pre-peak centered at 3 eV in whose inflexion point the zero of the energy scale (the edge energy) was fixed. For *3d*-metals with cubic crystal symmetry such as Ni, this pre-edge structure is due to electronic transitions from the *1s* level to a series of *p*-like empty energy states in the metal *d*-band, just above the Fermi level [12,13,20]. The hump at about 15-20 eV above the edge can be associated to electron excitations from the *1s* to higher energy *p*-states [13,20], but they may also correspond to the multi-scattering of the incident beam by nearly located atoms in the metal crystal, as specifically interpreted for Fe [14,21].

XANES at the Ni and Fe edges (Fig. 2 and 3) indicate a reduction of the pre-peak intensity and an enhancement of the 4p-hump in the spectra of both atoms in the codeposit, as compared to those of the bulk elements. This provides an indication that there is a difference in the electronic structure and/or crystalline symmetry in the alloy in comparison with the pure metals. On the other hand, the EXAFS results obtained at the Ni K edges (Fig. 4A) show that the coordination numbers (intensity of the magnitude of the Fourier transform) are smaller for the Ni-Fe alloy, compared to bulk Ni, in accordance with the formation of a rough surface material, as observed in Fig. 1. The FT features around 4 Å (Fig. 4) give evidences that the Fe atoms are preponderantly incorporated in the *fcc* structure of Ni, contrarily to the situation found in bulk Fe for which the crystal structure is body centered cubic (*bcc*).

The marked differences in the electronic properties and crystal symmetry of Ni atoms between the Ni-Cu-Fe alloy and pure Ni are certainly due to the coordination with Cu and Fe, but there is also a possibility that the changes of the edge features may come from the coordination of Ni or Fe with some oxi-hydroxides, and this can be discussed taking into account the XANES spectrum of Fe in a FeOOH sample shown in Fig. 3. Here, it is seen that the pre-peak is very weak, while the multi-scattering hump is very prominent, as usually observed for metal oxi-hydroxides [15-16]. The behavior is quite different from that of Fe in the Ni-Cu-Fe sample, indicating that the Fe atoms in the alloy are preponderantly in the metallic (reduced) form. By analogy, the same conclusion can be reached regarding the Ni atoms.

Electrochemical Characterization

With the aim to checking the stability of the bath solution and the reproducibility of the Ni-Cu-Fe codeposits, the electrodeposits were prepared using a fresh bath with pH 3.2 and also solutions that were left to stand for eight and fifteen days. The steady-state polarization curves for these Ni-Cu-Fe electrodes are shown in Figure 5. It can be seen that after 15 days the bath still maintains the plating properties and is capable of reproducing satisfactorily the electrodeposit, which behaves like a fresh bath. In this case, a very small amount of precipitate was observed in the solution after de electrodeposition procedure. Experiments carried out with solutions left to stand for more than 15 days showed a loss of activity of the deposits.

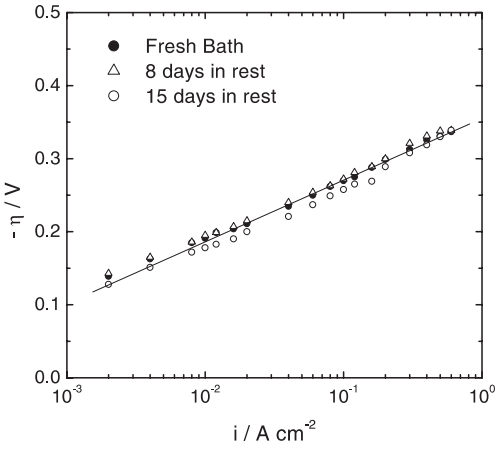

Figure 5. Tafel Plots for the *her* on electrodeposited Ni-Cu-Fe electrodes obtained in brine solution at 298K. The electrodes were prepared with the same bath but at different times after preparation, as indicated in the Figure.

The stability of the electrode material is also one of the important characteristics that must be established. Thus, the stability was tested through long term working experiments, by operating the electrode at a constant current density of 210 mA cm^{-2} at 298 K in brine solution. The

corresponding dependence of the overpotential *vs* time is presented in Figure 6, where it is observed that the Ni-Cu-Fe electrode is very stable in the time frame of the experiment (260 hours).

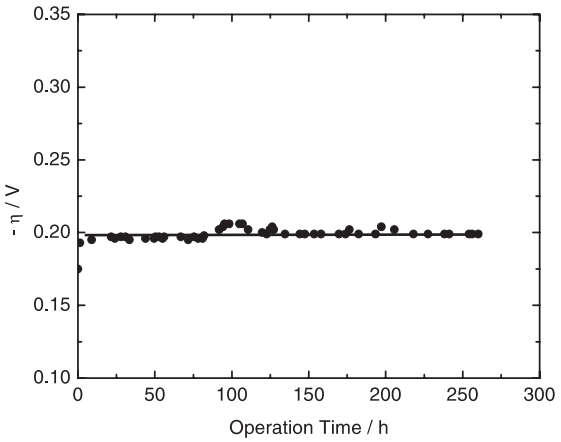

Figure 6. Continuous operation of the Ni-Cu-Fe electrode at 210 mA cm^{-2} in brine solution at 298 K.

In order to evaluate the effect of temperature on the electrocatalytic properties of the material, Tafel plots for the *her* were obtained in brine solution in the temperature range 298 - 353 K. These results are shown in Figure 7 and the corresponding electrochemical parameters for the *her* obtained from these plots are collected in Table 1. It is interesting to note that at all temperatures the steady-state polarization curves show only one Tafel slope in the current range 0.002 – 0.6 A cm^{-2}. This slope is almost independent of temperature, contradicting the predictions of classical theories. This phenomenon has been observed for other materials [5] and has been discussed in terms of the entropic and enthalpic components of the activation energy [23]. Also, this behavior is opposite to that observed by Carvalho et al.[4] for Ni-Fe, who found two Tafel slopes that had an inverse dependence with the temperature. From this, it can be concluded that the presence of Cu induces some modifications of the intrinsic electrocatalytic characteristics of the electrodeposited material.

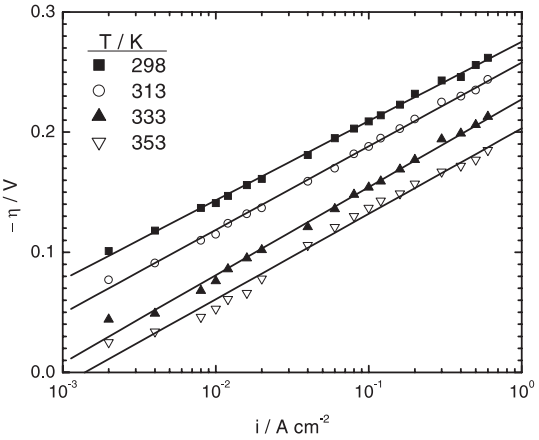

Figure 7. Tafel Plots for the *her* on Ni-Cu-Fe electrodes obtained in brine solution at different temperatures.

T / K	b / mV dec^{-1}	i_o / A cm^{-2}	$\eta_{210\ mA/cm^2}$ / V
298	66	6.65 x 10^{-5}	0.231
313	70	2.08 x 10^{-4}	0.210
333	73	8.03 x 10^{-4}	0.179
353	71	1.52 x 10^{-3}	0.155

Table 1. Tafel parameters for the *her* on the Ni-Cu-Fe electrode, obtained in brine solution. b: Tafel slope. i_o: exchange current density. h: overpotential.

With the values of the exchange current density (i_o) from Table 1, an Arrhenius plot was constructed and an activation energy for the *her* of 50.7 kJ mol^{-1} was obtained. This value is higher than that observed before for Ni-Fe [4] (35 kJ mol^{-1}), but is similar to those observed for bright [24] and porous nickel [25] (41 kJ mol^{-1} and 42 kJ mol^{-1} respectively), indicating similar catalytic activity. Analyzing the values of the overpotential measured at a current density of 210 mA cm^{-2}, an enhanced electrocatalytic activity to the *her* is observed for the Ni-Cu-Fe codeposit. At 353 K (the operational temperature used in industrial electrolysers) the overpotential for the Ni-Cu-Fe electrode is 249 mV lower than that of mild steel (404 mV), used in commercial unipolar electrolisers, and 19 mV lower than that of the previously obtained Ni-Fe material [4]. The values of the exchange current density (i_0) are higher for Ni-Cu-Fe compared to Ni-Fe and this indicates that the poor intrinsic

catalytic activity of this material is compensated by a larger improvement due to its larger surface area, as observed from the SEM and EXAFS measurements.

Conclusions

The stability of the electrodeposition baths developed to produce Ni-Cu-Fe surfaces is very high, when low pH´s are used, and these baths can be used to produce codeposits with high activity for the *her* in brine solutions. The mechanistic aspects of the reaction on Ni-Cu-Fe are different from those observed on Ni-Fe. In this sense, a positive aspect is the presence of only one Tafel slope in the whole current range investigated, in contrast with Ni-Fe. It is also found that the larger active surface area is the main factor responsible for the enhanced activity of this material. The X-ray absorption spectroscopy measurements showed that the Fe atoms are preponderantly incorporated in the *fcc* structure of Ni, contrarily to the situation in bulk Fe for which the crystal structure is body centered cubic (*bcc*) indicating the formation of a true alloy.

Acknowledgments. The authors wish to thank the Conselho Nacional de Desenvolvimento Científico e Tecnológico (CNPq), Fundação de Amparo à Pesquisa do Estado de São Paulo (FAPESP), and the Financiadora de Estudo e Projetos (FINEP), Brazil, for financial support.

M. J. Giz, M. C. Marengo, E. A. Ticianelli, E. R. Gonzalez. Caracterização física e eletroquímica da liga Ni-Cu-Fe para uso como cátodo de hidrogênio em células de cloro-soda.

Resumo: Este trabalho descreve o desenvolvimento de um banho alternativo de acetato para a codeposição eletroquímica de eletrodos de Ni-Cu-Fe em baixo pH, que é estável por várias semanas e produz eletrodos com bom desempenho para a eletrólise de cloro-soda. A caracterização física da superfície de eletrodo foi feita usando espectroscopia de absorção de raios X, microscopia eletrônica de varredura e análise dispersiva de energia. A avaliação do material como eletrocatalisador para a reação de desprendimento de hidrogênio (rdh) foi realizada em solução alcalina (160 g/L NaCl + 150 g/L NaOH) em diferentes temperaturas, através de curvas de polarização de estado estacionário. Os eletrodos de Ni-Cu-Fe obtidos com este banho apresentaram baixos sobrepotenciais para a rdh, em torno de 0.150 V a 353 K, e boa estabilidade sob condições de operação continuada por 260 horas. Um aspecto positivo deste cátodo é que o comportamento de polarização do material apresentou somente um coeficiente de Tafel no intervalo de temperatura de 298-353 K.

Palavras-chave: Produção de hidrogênio; cátodos; eletrólise; cloro-soda.

References

[1] S. Trasatti. Electrocatalysis of Hydrogen Evolution Progress in Cathode Activation. In: Gerischer, H. and Tobias, C. W. Advances in Electrochemical Science and Enginnering, Vol. 2, Weinheim, VCH, 1991.
[2] I. Arul raj, K. I. J. Vasu. *Appl. Electrochem.* 20 (1990)32.
[3] J. De Carvalho, G. Tremiliosi-Filho, L. A. Avaca, E. R. Gonzalez. *Int. J. Hydrogen Energy* 14 (1989) 161.
[4] J. De Carvalho, G. Tremiliosi-Filho, L. A. Avaca, E. R. Gonzalez. In S. Srinivasan, S. Wagner and H. Wroblowa (Eds.) Electrode Materials and Processes for Energy Conversion and Storage, The Electrochemical Society, Pennington, New Jersey, v.87-12, p.356, 1987.
[5] M. J. Giz, S. A. S. Machado, L. A. Avaca, E. R. Gonzalez. *J. Appl. Electrochem*. 22 (1992) 973.
[6] M. J. Giz, G. Tremiliosi-Filho, E. R. Gonzalez, S. Srinivasan, A. J. Appleby**.** *Int. J. Hydrogen Energy* 20 (1995) 423.
[7] M. J. Giz, S. C. Bento, E. R. Gonzalez. *Int. J. Hydrogen Energy* 25 (2000) 621.
[8] B. E. Conway, J. O´Bockris. *J. Chem. Phys*. 26 (1957) 532.
[9] J. M. Jaksic, N. V. Krstajic, B. N. Grgur, M. M. Jaksic. *Int. J. Hydrogen Energy* 23(1998) 667.
[10] J. McBreen, S. Mukerjee. *J. Electrochem. Soc*. 142 (1995) 3399.
[11] S. Mukerjee, S. J. Lee, E. A. Ticianelli, J. McBreen, B. N. Grgur, N. M Markovic, P. N. Ross, J. R. Giallombardo, E. S. De Castro. *Electrochem. Solid State Letters* 2 (1999) 12.
[12] J. McBreen. In Situ Synchrotron Techniques in Electrochemistry. In: Rubinstein, I. Physical Electrochemistry: Principles, Methods and Applications, Marcel Dekker Inc., NY,

Cap. 8, 1995.
[13] D. A. Tryk, I. T. Bae, Y. Hu, S. Kim, M. R. Antonio, D. A Scherson. *J. Electrochem. Soc*. 142 (1995) 824.
[14] E. A. Ticianelli, S. Mukerjee, J. McBreeN, G. D. Adzic, J. R Johnson, J. J. Reilly. *J. Electrochem. Soc*. 146 (1999) 3582.
[15] A. N. Mansour, C. A. Melendres, M. Pankuch, R. A. Brizzolara. *J. Electrochem. Soc*.141 (1994) L69.
[16]. A. N. Mansour, J. McBreen; C. A. Melendres. *J. Electrochem. Soc.* 146 (1999) 2799.
[17] H. Tolentino, J. C. Cezar, D. Z. Cruz, V. Compagnon-Caillol, E. Tamura, M. C. Alves. *J. Synchrotron Radiation* 5 (1998) 521.
[18] T. Ressler. *J. Phys IV* C2 (1997) 269.
[19]. J. B. A. D. Van Zon, D. C. Koningsberger, H. F. J. Van't Blik, D. E. Sayers. *J. Chem. Phys*. 82 (1985) 5742.
[20] R. J. Iwanowski, K. Lawniczak-Jablonska, Z. Golacki, A. Traverse. *Chem. Phys. Letters* 283 (1998) 313.
[21] V. G. Harris, K. M. Kemner, B. N. Das, N. C. Koon, A. E. Ehrlich, J. P. Kirkland, J. C. Woicik, P. Crespo, A. Ernando, A. Garcia Escorial. *Phys. Review B*. 54 (1996) 6929.
[22] I. Nakabayashi, E. NagaO, K. iyata, T. Moriga, T. Ashida, T. TomidA, M. Hyland, J. Metson. *J. Mater. Chem*. 5 (1995) 737.
[23] B. E. Conway, D. F. Tessier, D. P. Wilkinson. *J. Electrochem. Soc.* 134 (1989) 2486.
[24] B. E. Conway, L. Bai. *Int. J. Hydrogen Energy* 111 (1986) 533.
[25] H. Wendt, V. Plzak. *Electrochim. Acta* 28 (1983) 27.